

# FLUX TRANSPORT AND TAIL DYNAMICS DURING A PROLONGED SUBSTORM INTERVAL

S. E. Milan<sup>1\*</sup>, J. A. Wild<sup>2</sup>, B. Hubert<sup>3</sup>, C. M. Carr<sup>4</sup>, E. A. Lucek<sup>4</sup>,  
J. M. Bosqued<sup>5</sup>, J. F. Watermann<sup>6</sup>, and J. A. Slavin<sup>7</sup>

<sup>1</sup>*Department of Physics and Astronomy, Leicester University, Leicester LE1 7RH, U.K. \*Steve.Milan@ion.le.ac.uk*

<sup>2</sup>*Department of Communications Systems, Lancaster University, Lancaster LA1 4WA, U.K.*

<sup>3</sup>*Laboratory of Planetary and Atmospheric Physics, University of Liege, B-4000 Belgium.*

<sup>4</sup>*Department of Physics, Imperial College London, London SW7 2AZ, U.K.*

<sup>5</sup>*Centre d'Etude Spatiale des Rayonnements, CESR/CNRS, 31028 Toulouse Cedex, France.*

<sup>6</sup>*Danish Meteorological Institute, Lyngbyvej 100, DK-2100 Copenhagen, Denmark.*

<sup>7</sup>*Laboratory for Extraterrestrial Physics, NASA Goddard Space Flight Center, Greenbelt, Maryland, U.S.A.*

## ABSTRACT

We present multi-point observations of a substorm which took place on 29 August 2004. The near-Earth magnetotail dynamics were observed by Cluster C1 and Double Star TC1, in conjunction with observations of the Northern Hemisphere ionospheric convection flow from the Super Dual Auroral Radar Network (SuperDARN), of the Southern Hemisphere auroral morphology from the Wideband Imaging Camera of the Far Ultraviolet instrument onboard the Imager for Magnetopause-to-Aurora Global Exploration spacecraft (IMAGE FUV/WIC), and of ionospheric substorm currents from the Greenland magnetometer chain. Following the substorm growth phase, expansion phase onset results in the closure of open magnetic flux for 3 hours, prolonged by continued creation of open flux at the dayside. The 3-hour duration of the substorm was punctuated by 5 dipolarizations which we interpret as individual bursts of reconnection, each closing  $\sim 0.125$  GWb of flux. Associated with each dipolarization were auroral enhancements, convection enhancements and a step-wise poleward progression of the substorm current wedge. We derive the amount of open flux in the magnetosphere from observations of the ionospheric polar cap, along with the corresponding rates of dayside and night-side reconnection. From these we can model the changing length of the magnetotail and variations in its radius,

flaring, and lobe field strength during the course of the growth and expansion phases of the substorm. Despite the simplicity of this modeling, we demonstrate good agreement between predicted lobe field strength and the observations of Cluster.

## 1. INTRODUCTION

Substorms are an integral component of the capture and subsequent release of solar wind magnetic flux by the magnetosphere. This process, mediated by magnetic reconnection, topologically rearranges the field such that for southwards IMF closed terrestrial field lines near the subsolar point are opened to interconnect with the solar wind magnetic field, and are then swept antisunwards to accumulate in the magnetotail lobes [1].

Figure 1 shows a schematic of the magnetosphere. Solid arrowed lines show southwards-directed interplanetary magnetic field (IMF) lines which reconnected with the terrestrial field at A. Dotted arrowed lines show northward-directed IMF field lines that impinged on the magnetosphere but did not reconnect. From right to left the pattern of northward- and southward-directed field lines represents the time-history of the IMF as it arrived at the subsolar magnetopause. Those field lines

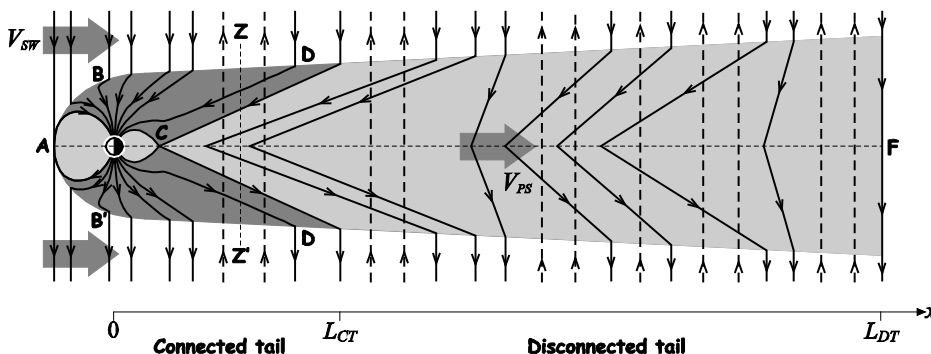


Figure 1. A schematic representation of the magnetosphere and its interaction with the IMF. Arrowed lines are magnetic field lines; these are solid if the IMF was southward and reconnected at the subsolar magnetopause, dotted if the IMF was northward, the field lines did not interact with the magnetosphere and slip about the dawn or dusk flank.

that reconnect (“open” field lines – dark grey region) are held hostage by the Earth and form the “connected” magnetotail; those that did not reconnect slip past the dawn or dusk flank. Eventually the open field lines are reconnected in the magnetotail at C, typically during a substorm, forming closed field lines at the Earthward end and releasing field lines back to the solar wind at the tailward end. These released field lines take some time to re-straighten, forming a structured wake downstream of the Earth known as the “disconnected” tail (light grey region). The distribution of disconnected field lines along AF indicates the time-history of reconnection in the tail.

Competition between dayside (A) and nightside (C) reconnection leads to changes in the proportion of terrestrial field lines that are open [2]. If dayside reconnection dominates then the proportion of open flux in the magnetosphere increases, known as the substorm growth phase. The region that this open flux maps to in the ionosphere, the polar cap, expands and the auroral oval moves to lower latitudes. Solar wind pressure acting on the magnetopause acts to maintain the magnetosphere in as streamlined a profile as possible. The rearrangement of the internal magnetic field and plasma that is required to maintain this profile results in magnetospheric and ionospheric convection [3]. As the flare of the magnetotail increases the internal pressure on the tail current layer eventually leads to the onset of magnetic reconnection and the closure of open flux; the attendant tail dynamics and auroral displays are known as the substorm expansion phase.

While the exact trigger for substorm onset is not yet understood, quantification of the reconnection rates on the dayside and nightside during the build up to and during the substorm give insights into this and are important in understanding the excitation of convection. Some progress has been made in determining statistically the amount of flux closed and the overall rate and duration of reconnection during substorms but the time-evolution of flux closure has been only sketchily examined [4, 5]. This paper studies one substorm, using Cluster and Double Star observations of the near-tail, IMAGE FUV observations of the aurora, SuperDARN measurements of the ionospheric flow, and Greenland magnetometers to determine the current systems. The aim is to gain an understanding of the reconnection evolution during an isolated substorm. Section 2 is a brief summary of a paper submitted to *Annales Geophysicae* [6]. In addition, in Section 3 we model the tail dynamics in response to the day- and nightside reconnection.

## 2. OBSERVATIONS

At the time of substorm expansion phase onset, ~02:20 UT, 29 August 2004, Cluster C1 and Double Star TC1 were located at  $X \approx -15$  and  $-9 R_E$ , respectively, both relatively near the  $Y = 0$  plane. Figure 2a and b present

$B_x$  and  $B_z$  components (GSM) of the magnetic field measured at C1, respectively, for 6 hours encompassing the substorm; panel c shows  $B_z$  from TC1, and panel h presents the  $B_z$  component of the IMF lagged to the magnetopause from ACE.

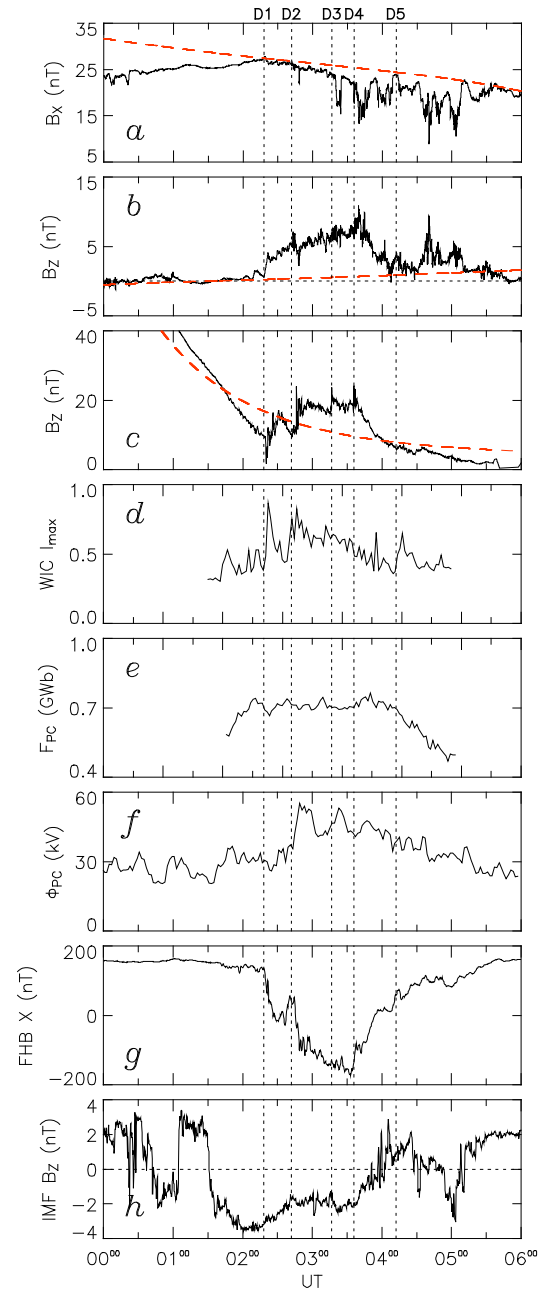


Figure 2. (a) and (b)  $B_x$  and  $B_z$  magnetic field components at Cluster C1; (c) Double Star TC1  $B_z$ ; (d) and (e) IMAGE FUV/WIC maximum brightness on the nightside (arbitrary units) and an estimate of  $F_{PC}$ ; (f) Transpolar voltage as measured by SuperDARN; (g) X-component magnetogram from the Greenland magnetometer chain; (h) IMF  $B_z$  measured at the ACE spacecraft, lagged to the magnetopause. Dipolarizations D1–5 are indicated by vertical dashed lines. T96 predictions of the field components measured by C1 and TC1 are indicated by dashed curves.

Superimposed on the magnetotail observations are predictions from the Tsyganenko T96 model. Cluster starts in the northern lobe, with the field mainly in the positive  $X$  direction. The field is depressed below the T96 prediction, but following a southward turning of the IMF at 00:40 UT it begins to increase and approaches T96 by 02:20 UT, the time of substorm expansion phase onset as determined from the auroral observations (see below). The increase in field marks the substorm growth phase, the loading of the tail lobes with new open flux due to subsolar reconnection at the dayside and the enhanced compression of the now-flared tail by the solar wind. As will be shown later, the amount of open flux in each lobe at the time of onset can be estimated at 0.7 GWb. At onset the field strength ceases to grow, indicating that flux is being removed from the central plane of the tail by magnetic reconnection. In fact, as the field strength roughly tracks the T96 prediction, which decreases with time as Cluster moves further down the tail, and does not diminish markedly below it (except for diamagnetic depressions due to encounters with the plasma sheet which will be described below), it would appear that the amount of flux in the lobes remains relatively constant, despite the tail reconnection. This is evidence that on-going dayside production of open flux is replenishing the lobes as rapidly as they are being emptied.

At substorm onset a dipolarization (D1, indicated by a vertical dashed line) was seen at both Cluster and Double Star. This enhancement of the  $B_z$  component of the field did not diminish for the next 90 mins. Indeed, at Double Star the  $B_z$  component increased in subsequent dipolarizations (D2 to D4). Shortly after each of these dipolarizations Cluster became engulfed by the plasma sheet (observed by CIS, though not shown for brevity), the enhanced plasma density leading to diamagnetic depressions in  $B_x$ , esp. after D3 and D4. At the northward turning of the IMF at 03:30–04:00 UT the  $B_z$  component in the tail decreases, perhaps indicating that the prolonged dynamics seen before were driven by continued loading of open flux at the dayside. A fifth dipolarization was seen at Cluster, though small now, at 04:10 UT; TC1 did not observe this as its orbit took it away from the region of interest.

Fig. 2d–g present a summary of the ionospheric observations during the substorm. Fig. 2g shows an  $X$ -component magnetogram from the Greenland magnetometer chain with a clear substorm bay; examination of magnetograms from the whole chain indicate several intensifications and a step-wise poleward progression of the substorm electrojet. Each of the intensifications and poleward steps matches closely the time of dipolarizations seen in the tail. Fig. 2d presents the maximum auroral brightness seen on the nightside by the WIC instrument on IMAGE. There is a first brightening at the time of the first dipolarization, though this is only short-lived. After D2 the auroral luminosity increases

again, and remains enhanced for the duration of the substorm. Detailed examination of the auroral images indicates that specific auroral events, including brightenings of the poleward boundary of the developing auroral bulge, can be associated with each subsequent dipolarization. Shown also is a calculation of the magnetic flux penetrating the dim portion of the ionosphere inside the auroral oval, the polar cap,  $F_{PC}$  (Fig. 2e); this is a proxy for the open flux in each magnetotail lobe. This increased during growth phase, as already inferred from the tail observations. Substorm onset occurred when the open flux reached 0.7 GWb.  $F_{PC}$  remained uniform while the IMF was southwards, indicating that dayside and nightside reconnection were balanced. After 04:00 UT when the IMF turned northwards, dayside reconnection ceased, nightside reconnection dominated and the polar cap shrank. Finally, the transpolar voltage deduced from the SuperDARN measurements is indicated in Fig. 2f. This was small at the beginning of the interval, and remained unchanged after the first dipolarization, but increased at D2. There were then subsequent intensifications of the convection at D3 and D4. The convection became small again some time after D5.

### 3. MODELLING

As demonstrated by [7], knowledge of the variations in  $F_{PC}$  during an interval allows the time history of dayside and nightside reconnection to be deduced. The dayside reconnection rate  $\Phi_D$  can be approximated by

$$\Phi_D = L_{eff} V_{SW} B_S \quad (1)$$

where  $V_{SW}$  is the solar wind velocity and  $B_S$  is the southward component of the IMF, such that  $V_{SW} B_S$  is the half-wave rectified  $Y$ -component of the motional electric field of the solar wind.  $L_{eff}$  is the effective length of the solar wind channel that reconnects with the magnetosphere, and must be determined by empirical means. Previous studies have shown that this tends to values near 20% of the cross-wind scale of the magnetosphere, that is 5–10  $R_E$ . The variability of  $L_{eff}$  between intervals of study is not understood, but  $L_{eff}$  appears to remain relatively constant for several hours during each period of interest. During the present interval we find that a value of  $L_{eff}$  of 12  $R_E$  best fits the observations (see below). If the day- and nightside reconnection rates are known, then changes in the open flux content of the magnetosphere are given by [2]

$$\frac{dF_{FC}}{dt} = \Phi_D - \Phi_N \quad (2)$$

If it is assumed, in the first instance, that  $\Phi_N = 0$  then the variation in  $F_{PC}$  can be found by combining Eqs. 1 and 2

and assuming some initial value for  $F_{PC}$ . This is shown in Figure 3. Panel (a) reproduces the variation in IMF  $B_z$  and panel (b) shows the dayside reconnection rate estimated from Eq. 1, using a value of  $L_{eff}$  of  $12 R_E$ . This has then been integrated in panel (c) to find the expected variation in  $F_{PC}$  (dotted curve). Superimposed on this is the measured  $F_{PC}$  from Fig. 2e.

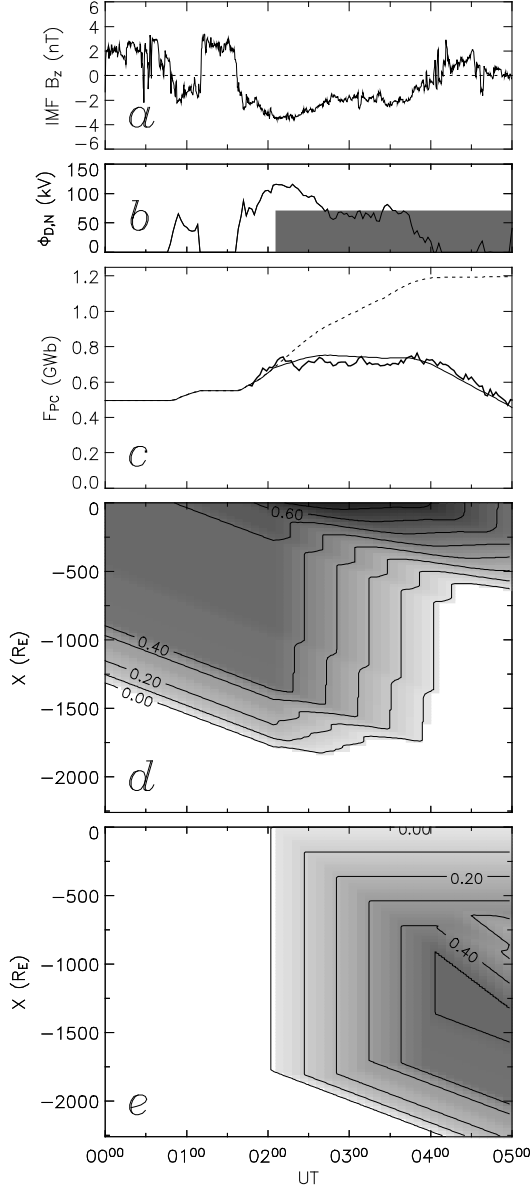


Figure 3. (a) The  $B_z$  magnetic field components at ACE lagged to the magnetopause; (b) Dayside and nightside reconnection rates derived from the observations of the polar cap size and interplanetary conditions; (c)  $F_{PC}$  derived from the auroral observations, and predicted polar cap size from dayside reconnection rate alone (dotted) and from dayside and nightside reconnection (full); (d) and (e) Modelled profiles of connected (open) flux in the magnetotail and disconnected flux (contours labelled in GWb).

The value of  $L_{eff}$  was determined by fitting the model trace with the observed growth in  $F_{PC}$  near 02 UT. At 02:10 UT the model and observed curves diverge, due to the onset of reconnection in the tail during substorm expansion phase. As described by [5], nightside reconnection appears to commence promptly at substorm onset and progresses at a relatively uniform level through to the recovery phase. The present example is no exception: by assuming that  $\Phi_N = 70$  kV from onset through to the end of the interval (represented by the grey box in Fig. 3b), the model trace (solid curve, Fig. 3c) reproduces well the observed variation in  $F_{PC}$ . The 70 kV nightside reconnection rate is sufficient to offset the dayside reconnection prior to 04 UT, such that  $F_{PC}$  remains constant, and then accounts for the deflation of the polar cap once dayside reconnection ceases at the northward turning of the IMF after 04 UT. The observations indicate that magnetic reconnection in the tail continues unabated for at least 3 hours, equivalent to the period of elevated auroral luminosities.

Knowing  $F_{PC}$  and the derived values of  $\Phi_D$  and  $\Phi_N$  allows us to determine the profiles of connected and disconnected magnetic flux within the magnetotail, as described by [7]. This is based on the simple premise that the open flux observed in the polar cap maps into the magnetotail lobe, but then reduces with down-tail distance  $x$  as field lines cross into the solar wind across the tail magnetopause (e.g. points D in Fig. 1). The amount of flux that is crossing the magnetopause at a down-tail distance  $x$  at time  $t$  is related to the rate of dayside reconnection that was ongoing at the time that the field lines were originally opened, i.e. at a time  $t - x/V_{SW}$ . This allows the profile of connected flux to be formulated as follows:

$$F_{CT}(x, t) = F_{PC}(t) - \frac{1}{V_{SW}} \int_0^x \Phi_D(t - x/V_{SW}) dx. \quad (3)$$

$F_{CT}(x, t)$  is then the connected flux crossing the plane  $X = -x$  (e.g. ZZ' in Fig. 1) for either  $Z > 0$  or  $Z < 0$ , i.e. in either the northern or southern lobe. The connected flux calculated in this manner is shown in Fig. 3d. The disconnected tail comprises field lines that have been released back to the solar wind by nightside reconnection but which haven't yet had time to recoil down the length of the tail. The profile of disconnected flux (Fig. 3e) can be found in a similar manner to the connected flux, though now the nightside reconnection rate must also be taken into account. First the total flux is calculated:

$$F_T(x, t) = F_{PC}(t) - \frac{1}{V_{SW}} \int_0^x \Phi_D(t - x/V_{SW}) dx + \frac{1}{V_{PS}} \int_0^x \Phi_N(t - x/V_{PS}) dx, \quad (4)$$

where  $V_{PS}$  is the speed of down-tail propagation in the plasma sheet; for simplicity we have taken  $V_{PS} = 2V_{SW}$ . The disconnected flux is then found from Eqs. 3 and 4:

$$F_{DT}(x,t) = \begin{cases} F_T(x,t) - F_{CT}(x,t), & F_{CT}(x,t) > 0 \\ F_T(x,t), & F_{CT}(x,t) < 0 \end{cases} \quad (5)$$

The calculations show a connected tail that is initially  $1300 R_E$  in length, which then grows to be  $1800 R_E$  long as the field lines are stretched by the flow of the solar wind. At the onset of reconnection in the tail the oldest open field lines, those which have been stretched longest by the solar wind, become part of the disconnected tail. These highly-kinked field lines initially stretch the full length of the tail and hence  $F_{DT}$  becomes non-zero between  $x = 0$  and  $1800 R_E$ , but recoil at a speed somewhat greater than the solar wind speed, such that the kink eventually catches up with the ends embedded in the solar wind (which are themselves constantly moving antisunwards). After the onset of the substorm, the open flux of the tail is gradually eroded until by 04 UT only recently opened field lines remain, these field lines being only  $\sim 700 R_E$  in length. By the same process, new disconnected field lines are being constantly added to the tail during the nightside reconnection burst, so the  $F_{DT}$  remains elevated through to the end of the substorm. It is clear that the substorm significantly alters the structure of the tail.

Finally, it is possible to use the profile of flux in the tail to study the pressure balance between the solar wind plasma and the internal magnetic pressure of the tail. We employ an approach similar to that of [8] to determine the shape of the tail magnetopause, in which the tail is considered to be roughly cylindrical in shape, though varying in radius (flaring) with down-tail distance. The aim of the modelling is to determine the variation of the tail radius  $R_T$ , lobe field strength  $B_L$ , and angle of flare  $\alpha$  with  $x$ . Reference [9] used similar arguments to determine when the tail magnetopause should move outward or inward over a spacecraft, i.e. determine variations in the tail radius; here we compare the predicted lobe field strength with the observations at Cluster. Pressure balance between solar wind ram pressure  $\rho V_{SW}^2$ , solar wind gas and magnetic pressures, bundled together as  $p_0$ , and the magnetic pressure presented by the lobe field  $B_L^2/2\mu_0$  can be written as

$$p_0 + 2\rho V_{SW}^2 \sin^2 \alpha = \frac{B_L^2}{2\mu_0} \quad (6)$$

where  $\rho$  is the solar wind density. The second term represents the stress normal to the magnetopause exerted by reflection of solar wind plasma from the boundary. Given  $\rho V_{SW}^2$ ,  $p_0$  and  $B_L$ , Eq. 6 can be solved

to find  $\alpha$ . This in turn allows the increase in radius of the tail to be determined:

$$\frac{dR_T}{dx} = \tan \alpha \quad (7)$$

Finally, knowing the tail radius and its flux content (both connected and disconnected) at  $x$ , derived from Eqs. 3–5, allows the lobe field strength to be determined, assuming that the tail is circular in cross-section:

$$B_L = \frac{2(F_{CT} + F_{DT})}{\pi R_T^2} \quad (8)$$

Reference [8] solved Eqs. 6–8 analytically, assuming that the flux content of the tail is a constant with  $x$ . We on the other hand solve them by iterating in  $x$ , as our flux model suggests the flux content varies with  $x$ . It is necessary to provide an initial boundary condition, which we take to be  $R_T = 12.5 R_E$  at  $x = 0$ . Figure 4 shows the results of these calculations, concentrating on the near-Earth portion of the tail. Fig. 4a and b show  $B_L$  (nT) and  $R_T$  ( $R_E$ ), respectively, with the dashed lines indicating the location of Cluster. Between 02 and 04 UT both the lobe field strength and the tail radius are enhanced, due to the high proportion of open flux  $F_{PC}$  in the magnetosphere. Fig. 4c compares  $B_L$  derived from the model at the location of Cluster (dotted curve) with actual measurements of the total field strength  $B_T$  made by Cluster. During the growth phase of the substorm, before 02:20 UT, excellent agreement between model and observations is found, with increases and decreases in magnetic field strength in response to south and north turnings of the IMF being reproduced faithfully by the model. The apparent decrease in the lobe field strength during the northward-turning of the IMF, 01:10 to 01:40 UT, is a consequence of a pause of the growth phase, coupled with the down-tail motion of the spacecraft towards a region where the tail is less flared and the field strength is lower. After substorm onset the correspondence is not so good, partially as a consequence of the approach of Cluster to the plasma sheet and diamagnetic drop-outs in the field strength.

#### 4. DISCUSSION AND CONCLUSIONS

The magnetotail lobes comprise those field lines which are open to the solar wind and which are stretched to great lengths by the flow of the solar wind while they remain connected to the Earth. Measuring the size of the footprint of these field lines in the ionosphere—the polar cap—allows the open flux content of the magnetosphere to be determined, from which can be deduced much of the large-scale structure and dynamics of the magnetotail. Structure and dynamics are modulated by the rates of dayside and nightside reconnection, the

former of which is related to upstream solar wind conditions, the latter by the need to remove open flux from the system once the stress in the magnetotail becomes too great to sustain. The specific trigger for the onset of reconnection in the tail is not yet understood. However, studies which aim to quantify the amount of open flux in the tail at substorm onset, and the rate and duration of the subsequent reconnection, e.g. [5], will help understand this. The present paper has studied the evolution of flux closure during one substorm when the Cluster and Double Star spacecraft were located in the magnetotail, such that the resulting dynamics could be investigated. A substorm growth phase is observed, the rate of growth of the polar cap suggesting a dayside reconnection rate of  $\sim 70$  kV. The magnetic field strength in the lobe increases during this period as open flux accumulates, leading to an outward flaring of the tail and the correspondingly increased stress applied to the tail magnetopause by the flow of the solar wind. Modelling the magnetopause shape accurately reproduces the internal field strength required to stand-off the solar wind.

Observations of the size of the polar cap indicate that following expansion phase onset the open flux content remains constant, indicating that dayside and nightside reconnection rates must be roughly equal at 70 kV. The polar cap does not contract until there is a northward turning of the IMF, such that dayside production of open flux ceases. The rate of contraction of the polar cap indicates that nightside reconnection continues at an unabated rate of  $\sim 70$  kV for at least 3 hours. In this time the Double Star observations show five clear dipolarizations, which we interpret as individual bursts of reconnection. It is possible that the first dipolarization is associated with reconnection of the closed flux of the plasma sheet, whereas the subsequent 4 dipolarizations are closure of open flux, though we have skirted this issue in the present paper for brevity. Approximately 30 mins occurs between dipolarizations, such that each must be responsible for the closure of  $\sim 0.125$  GWb of flux. Overall  $\sim 0.6$  GWb of flux are closed during the substorm's 3-hour duration, equivalent to the amount of open flux in a typical polar cap. The transport of open flux across the polar cap should occur at a rate of 70 kV when both dayside and nightside reconnection are active; the SuperDARN measurements of the transpolar voltage indicate a value nearer 50 kV. We believe that the discrepancy arises due to sparse radar backscatter in some portions of the polar cap, leading to an underestimate of the true voltage. Associated with each of the dipolarizations observed in the tail there are auroral signatures, magnetic substorm bays, and enhancements in the convection voltage. Each dipolarization sees a step-wise poleward motion of the substorm current wedge. This tallies with an enhanced value of  $B_z$  at both Cluster and Double Star from onset until 04:00 UT, indicating flux pile-up in the near-Earth tail. We believe that each subsequent burst of reconnection causes the pile-up region to extend further down-tail, with an attendant

poleward motion of the associated auroral signatures. The flux pile-up only diminished once the IMF turned northwards, and dayside reconnection ceased. This suggests that even after substorm onset as the nightside reconnection rate did not exceed that at the dayside the substorm was unable to relieve the stress in the tail, or in other words, the substorm was prolonged by the ongoing dayside opening of flux. The factors which govern the rate at which reconnection progresses in the tail are not yet known, though the reconnection rate appears to be able to take a wide range of values [5]. Clearly, the competition between dayside and nightside reconnection are of fundamental importance in determining the duration and evolution of a substorm.

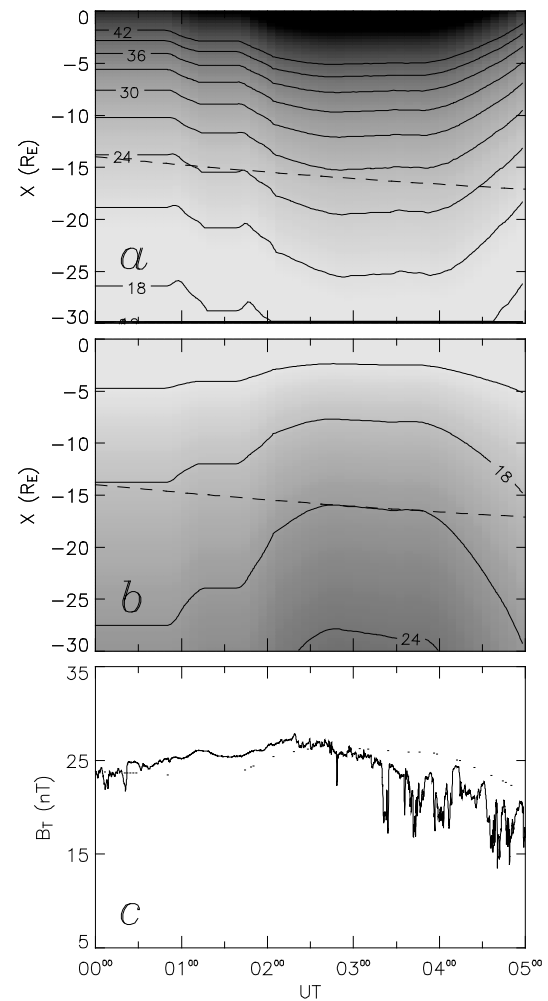


Figure 4. (a) Modelled variation in lobe field strength (contours in nT), dashed line indicating location of Cluster; (b) Modelled tail radius ( $R_E$ ); (c) Total magnetic field strength from Cluster, with model prediction superimposed (dots).

The length of the magnetotail can be calculated from observations of  $F_{PC}$  and the reconnection rates, and this indicates that the open flux region of the tail shrinks from a length of  $1800 R_E$  to approximately  $800 R_E$  dur-

ing the substorm. The flux disconnected during the substorm can also be predicted, and could be compared with observations of the tail dynamics at distances further down the tail if spacecraft were present there.

The present study has demonstrated the utility of combining ground- and space-based observations of the near-Earth magnetosphere for the study of large-scale solar wind-magnetosphere coupling. Future work will concentrate on investigating the relationship between nightside and dayside reconnection during more events.

#### ACKNOWLEDGEMENTS

This study was conducted under the auspices of the Cluster and Double Star Ground-Based Working Group. Cluster analysis at Imperial College is supported by PPARC. EAL is supported by a PPARC fellowship. The authors would like to thank N. F. Ness and D. J. McComas for the provision of data from ACE MFI and ACE SWEPAM, respectively.

#### REFERENCES

1. Dungey J. W., Interplanetary magnetic fields and the auroral zones, *Phys. Rev. Lett.*, 6, 47-48, 1961.
2. Siscoe G. L. and Huang T. S., Polar cap inflation and delation, *J. Geophys. Res.*, 90, 543, 1985.
3. Cowley S. W. H. and Lockwood M., Excitation and decay of solar wind-driven flows in the magnetosphere-ionosphere system, *Ann. Geophysicae*, 10, 103-115, 1992.
4. Milan S. E., Lester M., Cowley S. W. H., Oksavik K., Brittnacher M., Greenwald S. W. H., Sofko G., and Villain J.-P., Variations in polar cap area during two substorm cycles, *Ann. Geophysicae*, 21, 1121-1140, 2003.
5. Milan S. E., Wild J. A., Grocott A., and Draper N. C., Space- and ground-based investigations of solar wind-magnetosphere-ionosphere coupling, *Adv. Space. Res.*, in press, 2005.
6. Milan S. E., Wild J. A., Hubert B., Carr C. M., Lucek E., Bosqued J. M., Watermann J. F., and Slavin J. A., Flux closure during a substorm observed by Cluster, Double Star, IMAGE FUV, SuperDARN, and Greenland magnetometers, *Ann. Geophysicae*, submitted, 2005.
7. Milan S. E., A simple model of the flux content of the distant magnetotail, *J. Geophys. Res.*, 109, A07210, 2004.
8. Coroniti F. V. and Kennel C. F., Changes in magnetospheric configuration during the substorm growth phase, *J. Geophys. Res.*, 77, 3361, 1972.
9. Milan, S. E., S. W. H. Cowley, M. Lester, D. M. Wright, J. A. Slavin, M. Fillingim, C. W. Carlson and H. J. Singer, Response of the magnetotail to changes in open flux content of the magnetosphere, *J. Geophys. Res.*, 109, A04220, 2004.